Electronic Supplementary Information

Fabrication of Inorganic-Organic Core-Shell Heterostructure: Novel CdS@g-C_3N_4 Nanorod Arrays for Photoelectrochemical Hydrogen Evolution

Yuangang Li*, Xiaoliang Wei, Huajing Li, Rongrong Wang, Juan Feng, Hui Yun and Anning Zhou*

College of Chemistry and Chemical Engineering, Xi'an University of Science and Technology, Xi'an 710054, P. R. China.
Corresponding author. Tel. /Fax: +86 29 85583183;
**E-mail: chemliyg@gmail.com (Y. L.)； psu564@139.com (A. Z.)*

Contents list:

Fig. S9 Enlarged TEM image of the CdS@g-C_3N_4 CSNRs.

Fig. S10 XRD pattern of blank FTO substrate.

Fig. S11 Photocurrent density versus potential curves for pure g-C_3N_4 in an aqueous solution containing 0.35 M Na_2SO_3 and 0.25 M Na_2S (pH=12) under (100 mW/cm^2 AM 1.5G) illumination.

Fig. S12 The incident photon to current efficiency (IPCE) was measured based on a monochromator (Zolix Instruments, China) in an aqueous solution containing 0.35 M Na_2SO_3 and 0.25 M Na_2S (pH=12) at 0.9 V versus RHE. The generated photocurrent signals were collected using a lock-in amplifier (standford instrument SR830 DSP) synchronized with a light chopper (standford instrument SR540). IPCE was calculated according to following equation:[1]

$$IPCE(\%) = [\frac{1240I(\lambda)}{\lambda J_{light}(\lambda)}] \times 100\%$$

where λ is the incident light wavelength, $I(\lambda)$ and $J_{light}(\lambda)$ are the corresponding measured photocurrent density and the recorded irradiance intensity at the specific wavelength of λ, respectively.

Fig. S13 Photocurrent density versus potential curves for different deposition times of g-C_3N_4 onto CdS NRs in an aqueous solution containing 0.35 M Na_2SO_3 and 0.25 M Na_2S (pH=12) under (100 mW/cm^2 AM 1.5G) illumination.

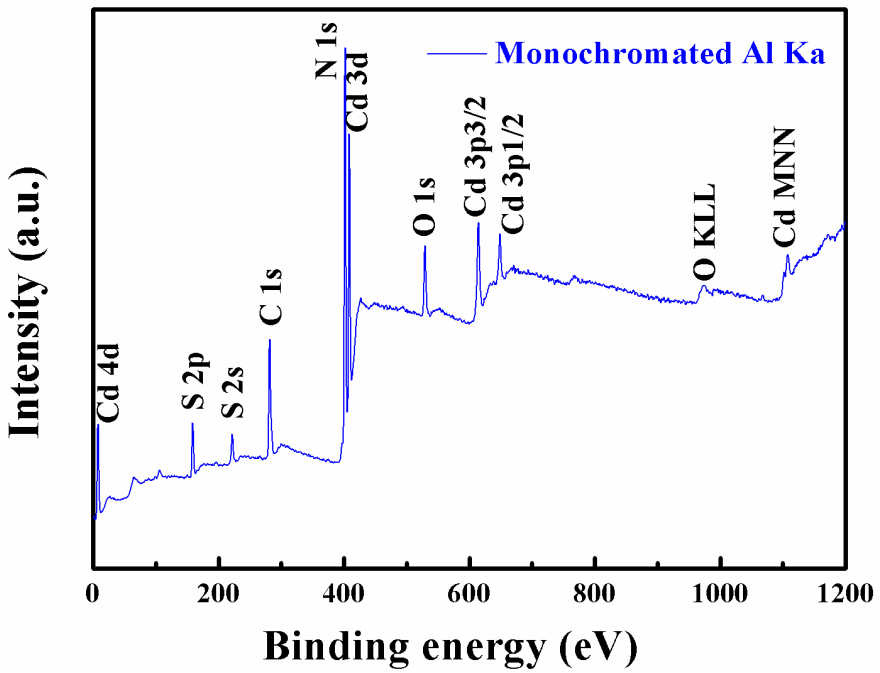

Fig. S1 XPS spectrum of the CdS@g-C_3N_4 CSNRs.

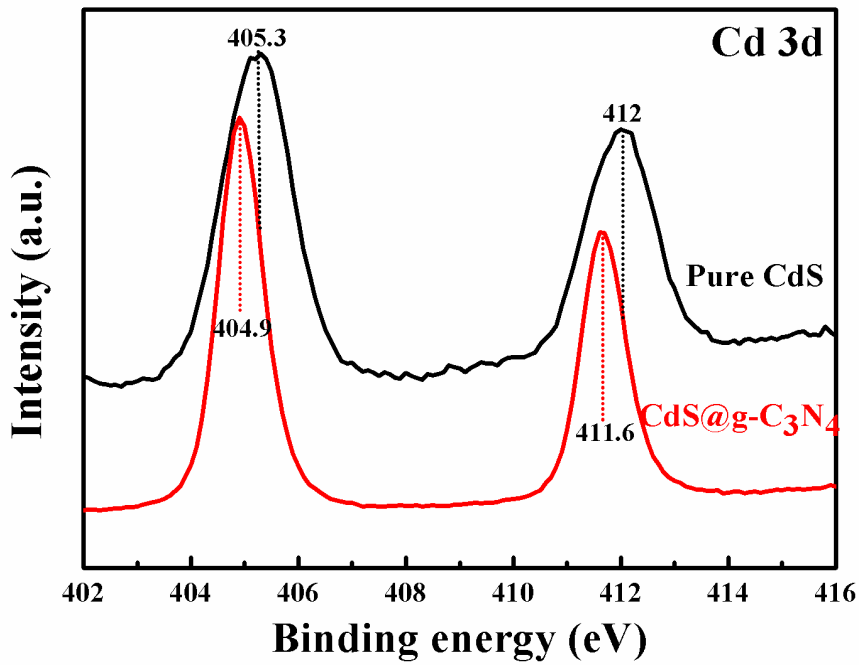

Fig. S2 XPS spectra of Cd 3d for pure CdS NRs and the CdS@g-C_3N_4 CSNRs.

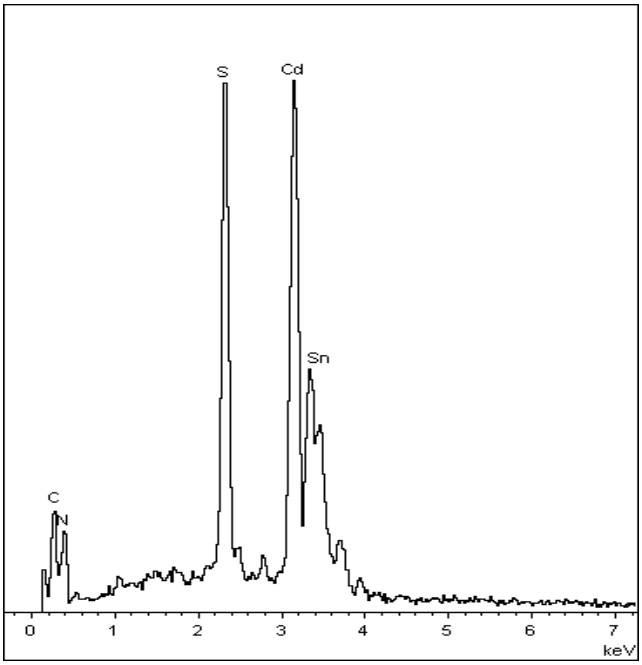

Fig. S3 EDX spectrum of the CdS@g-C_3N_4 CSNRs.

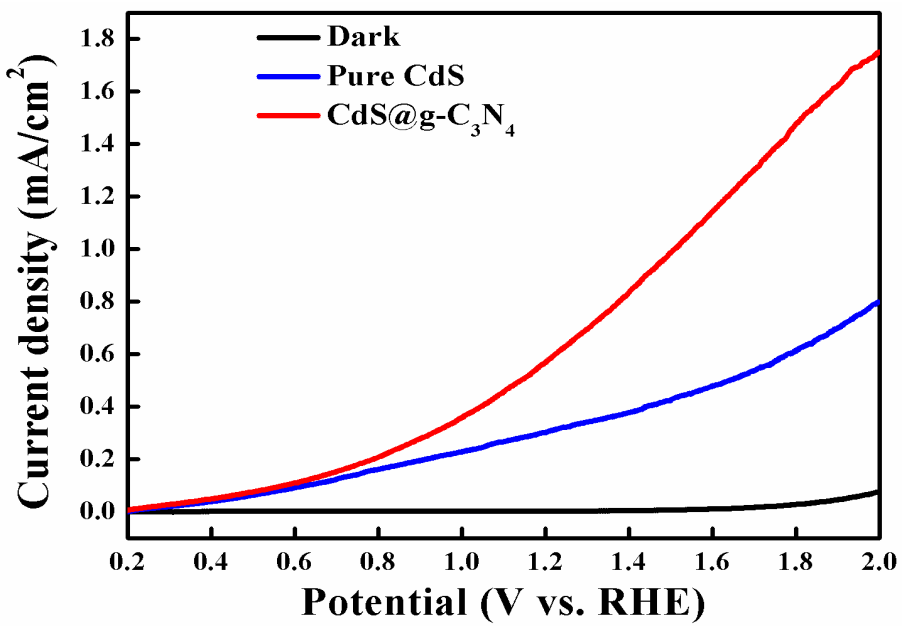

Fig. S4 Photocurrent density versus potential curves for CdS NRs and CdS@g-C_3N_4 CSNRs in a 0.2 M Na_2SO_4 (pH=6.8) aqueous solution under (100 mW/cm^2 AM 1.5G) illumination.

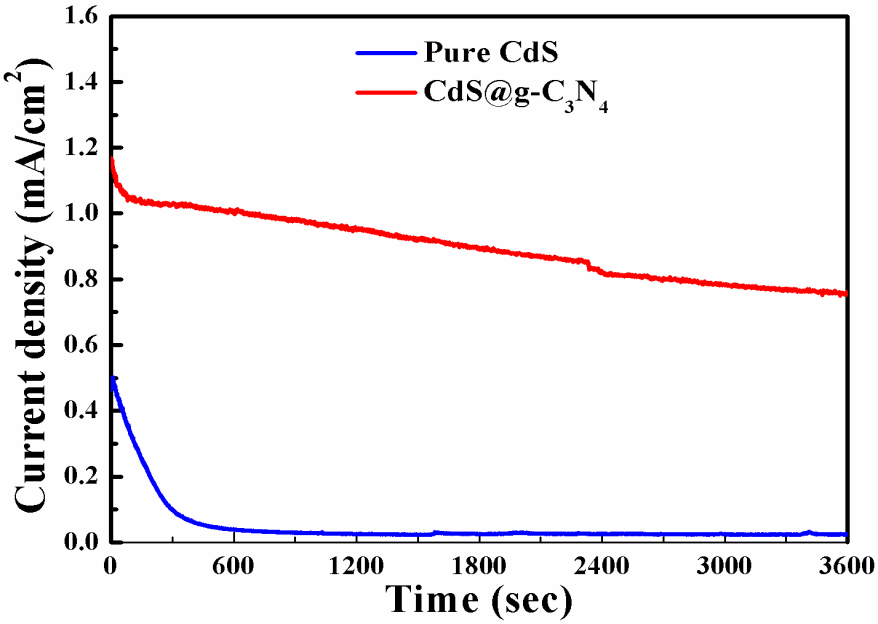

Fig. S5 Photostability measurements of CdS NRs and CdS@g-C_3N_4 CSNRs in a 0.2 M Na_2SO_4 (pH=6.8) aqueous solution under continuous (100 mW/cm^2 AM 1.5G) illumination for one hour at 1.6 V versus RHE.

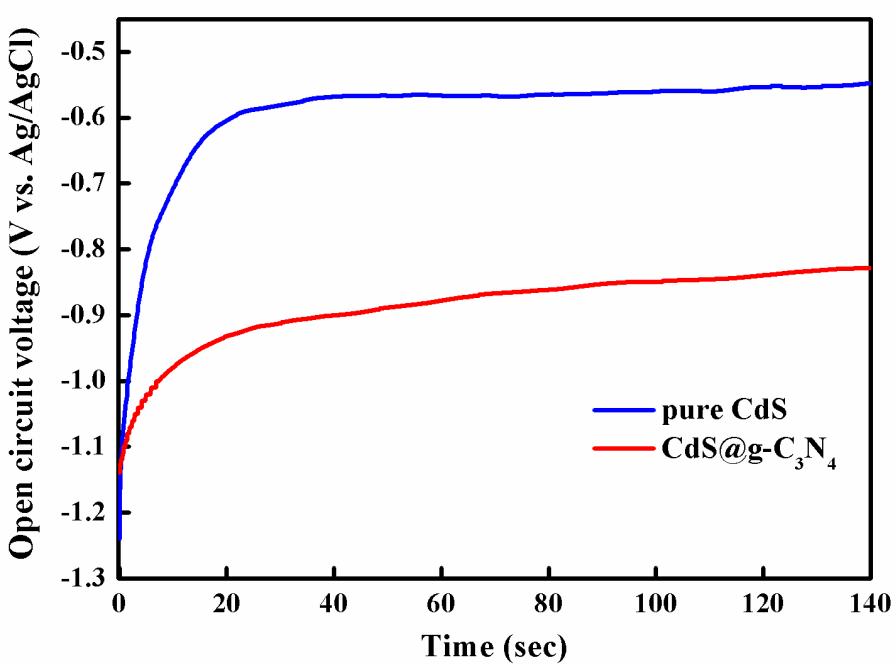

Fig. S6 Open circuit voltage decay with time for CdS NRs and CdS@g-C_3N_4 CSNRs after illumination interruption.

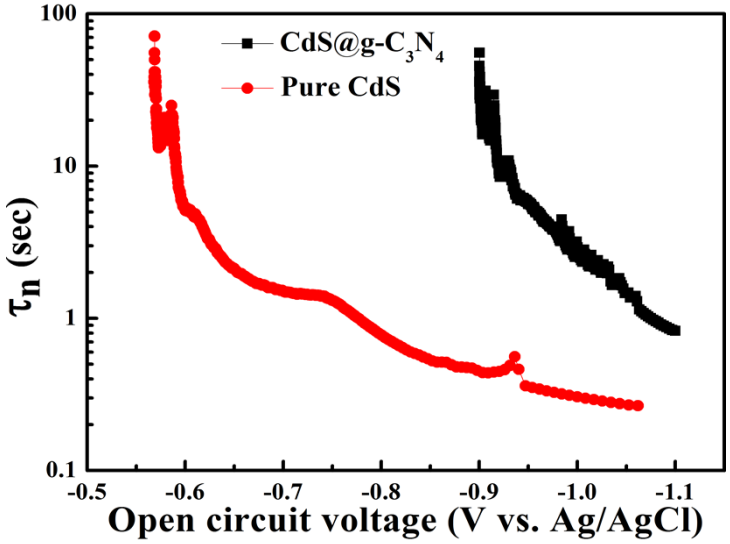

Fig. S7 Comparison of the lifetime of electrons derived from the given equation as a function of open circuit voltage decay.

Note: Open circuit voltage decay measurements were conducted to further examine effective charge separation and the lifetime of electrons. As revealed in **Fig. S11**, Analysis of open circuit voltage decay showed that CdS@g-C_3N_4 CSNRs heterostructure alleviated open circuit voltage decay compared with pure CdS NRs. Furthermore, we also studied electron lifetime by the following model equation:[2]

$$\tau = -\frac{K_B T}{e}\left(\frac{dV_{OC}}{dt}\right)^{-1}$$

where k_B is Boltzmann's constant, T is the temperature, V_{oc} is the open circuit voltage, and e is the elementary charge. As presented in **Fig. S12**, the calculated results show that CdS@g-C_3N_4 CSNRs heterostructure exhibit a much higher lifetime of electrons with a lower recombination rate as compared to pure CdS NRs. This phenomenon further demonstrates that efficient charge separation is obtained in the CdS@g-C_3N_4 CSNRs heterostructure.

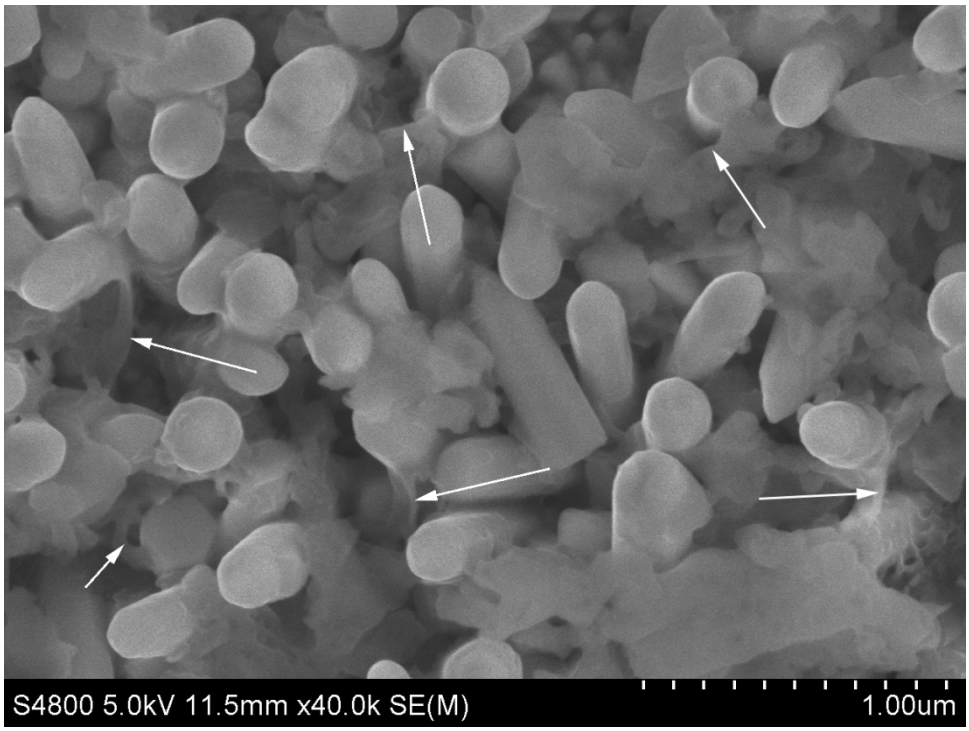

Fig. S8 Enlarged SEM image of the CdS@g-C_3N_4 CSNRs (g-C_3N_4 sheets are marked by white arrows).

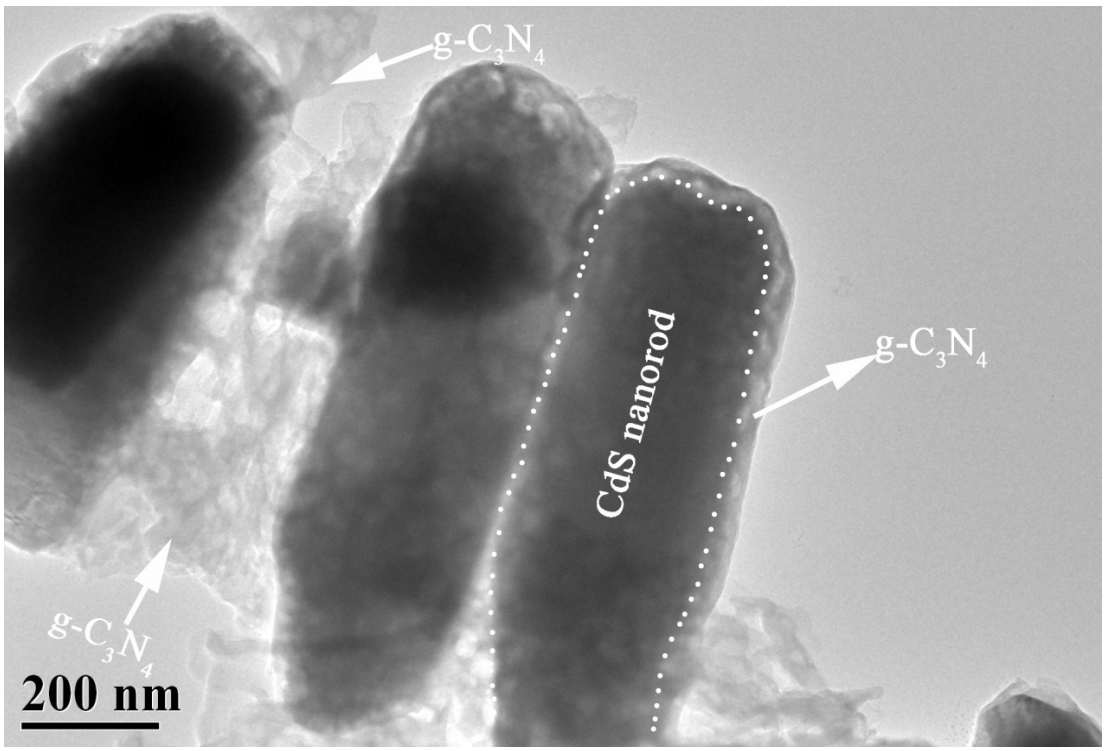

Fig. S9 Enlarged TEM image of the CdS@g-C_3N_4 CSNRs.

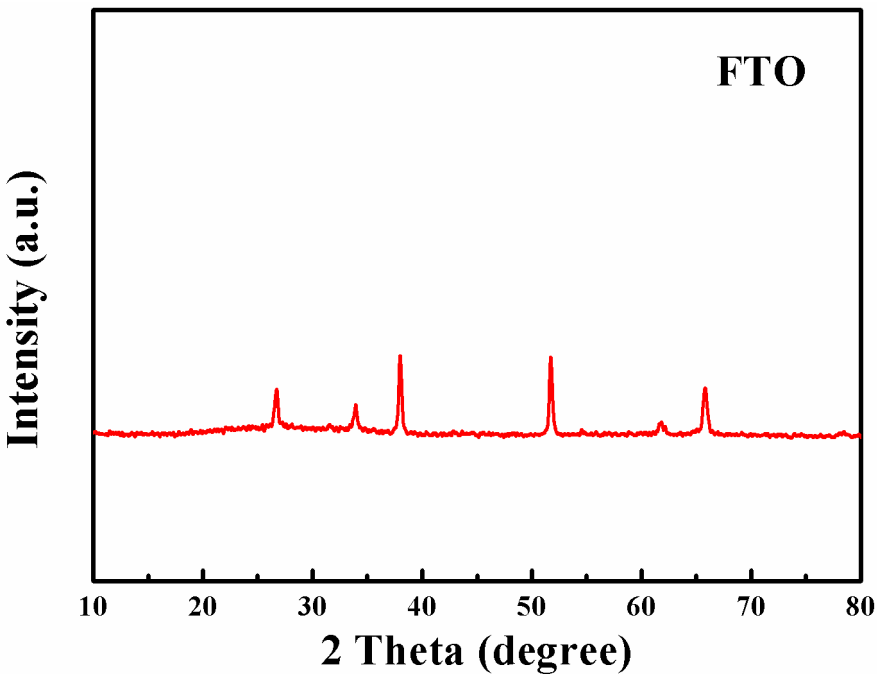

Fig. S10 XRD pattern of blank FTO substrate.

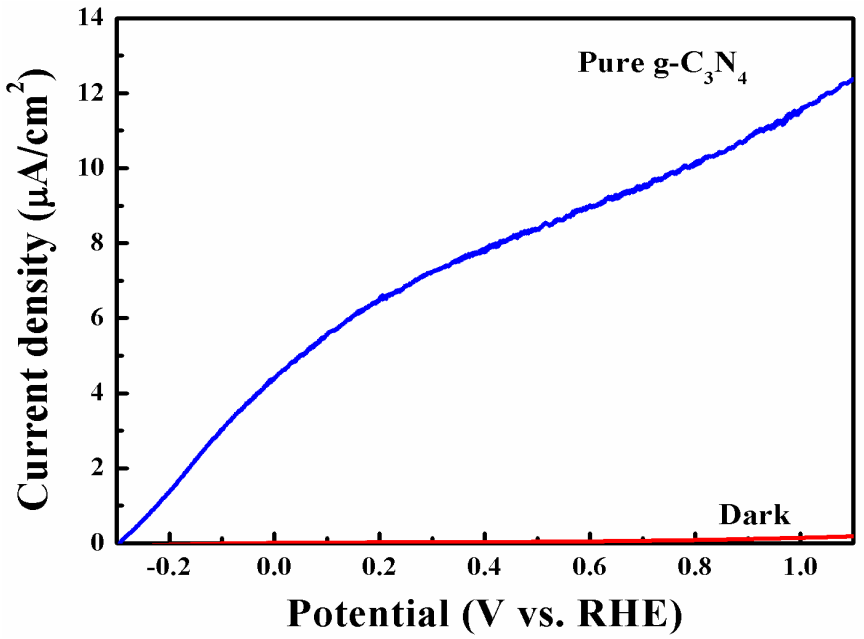

Fig. S11 Photocurrent density versus potential curves for pure g-C_3N_4 in an aqueous solution containing 0.35 M Na_2SO_3 and 0.25 M Na_2S (pH=12) under (100 mW/cm^2 AM 1.5G) illumination.

Note: Pure g-C_3N_4 shows a much smaller photocurrent density (the maximum of photocurrent density is 12.3 μA/cm^2).

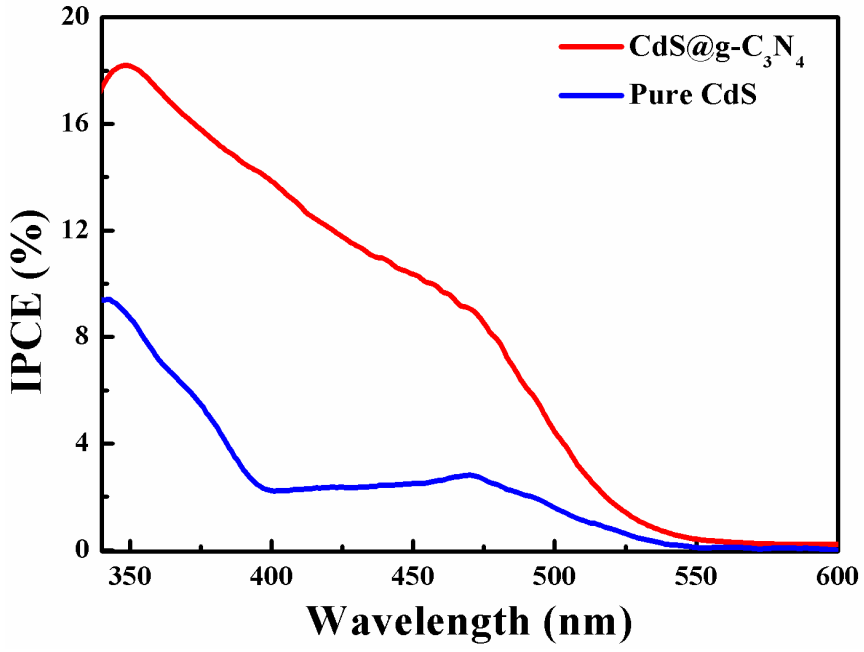

Fig. S12 Incident photon to current efficiency (IPCE) of CdS NRs and CdS@g-C_3N_4 CSNRs.

Note: Fig. S10 shows IPCE spectra of CdS NRs and CdS@g-C_3N_4 CSNRs. Pure CdS NRs shows rising IPCE from 530 nm in agreement with bandgap. The IPCE of CdS@g-C_3N_4 CSNRs is higher than that of CdS NRs across the visible light

absorption range, which indicates that photogenerated electron-hole pairs are efficiently separated in the CdS@g-C_3N_4 CSNRs heterostructure.

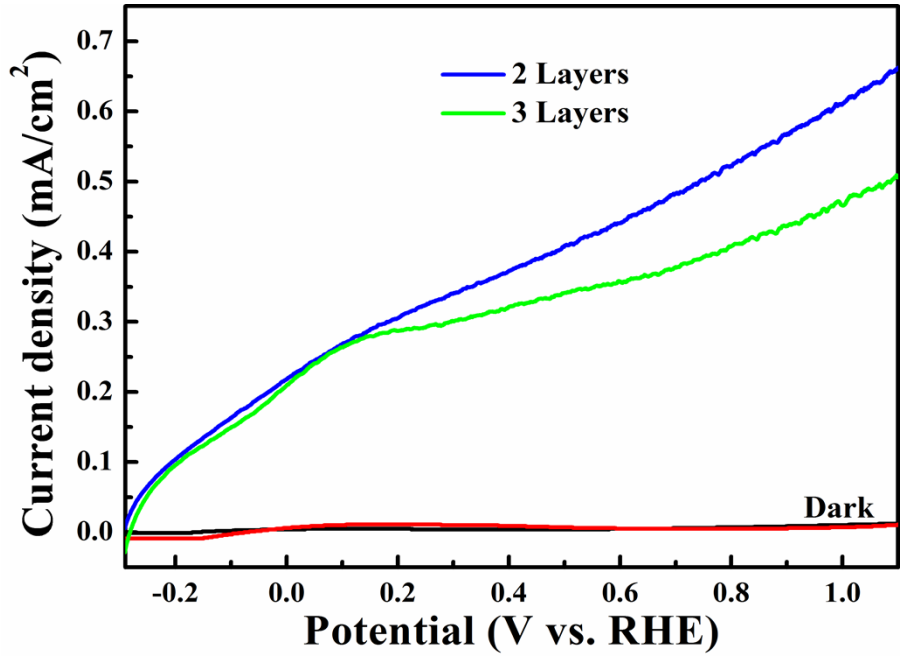

Fig. S13 Photocurrent density versus potential curves for different deposition times of g-C_3N_4 onto CdS NRs.

Note: Photocurrent density versus potential curves for different deposition times of g-C_3N_4 onto CdS NRs also were measured in an aqueous solution containing 0.35 M Na_2SO_3 and 0.25 M Na_2S (pH=12) under (100 mW/cm^2 AM 1.5G) illumination. As shown in **Fig.S13**, as the deposition times increase, the CdS@g-C_3N_4 CSNRs show decreased Photocurrent density, which possibly due to the light-filtering effect and low conductivity of g-C_3N_4.[3]

references

1. J. Li, S. K. Cushing, P. Zheng, T. Senty, F. Meng, A. D. Bristow, A. Manivannan and N. Wu, J. Am. Chem. Soc., 2014, 136, 8438-8449.

2. J. H. Bang and P. V. Kamat, Adv. Funct. Mater., 2010, 20, 1970-1976.

3. Z. Huang, Q. Sun, K. Lv, Z. Zhang, M. Li and B. Li, Appl. Catal., B, 2015, 164,420-427.